12-PULSE RECTIFIER WITH TWO DCM BOOST-TYPE HALF-CONTROLLED BRIDGES FOR VARIABLE-INPUT-FREQUENCY APPLICATIONS

João Carlos Pelicer Junior[1], Angelo César de Lourenço[2], Luis De Oro Arenas[3], Falcondes José Mendes de Seixas[4]

[1]Federal Institute of São Paulo - IFSP, Sorocaba - SP, Brazil

[2]Federal Institute of Education, Science, and Technology of Mato Grosso do Sul, Campo Grande - MS, Brazil

[3]São Paulo State University, Institute of Science and Technology of Sorocaba, Sorocaba - SP, Brazil

[4]São Paulo State University, Ilha Solteira - SP, Brazil

e-mails: joao1.pelicer@gmail.com, angelo.lourenco@ifms.edu.br, luis.arenas@unesp.br, falcondes.seixas@unesp.br

***Abstract* – This paper presents the analysis of the integration of two three-phase half-controlled boost converters, operating in discontinuous conduction mode (DCM), to the auto-connected 12-pulse rectifier. The proposed structure shows a reduced current harmonic content compared to the traditional 12-pulse rectifiers, being a simpler and effective alternative to using rectifiers with higher pulse numbers. It also presents a greater range of possibilities for regulating the output voltage, without the use of synchronization algorithms or rigorous control techniques, being possible to send to all controlled switches, the same command signal, resulting in a simpler logic. Another advantage of using the proposed technique is the employment of a single-loop voltage control scheme, reducing the computational and financial cost by eliminating some elements such as current sensors. Moreover, the proposed strategy provides soft commutations (Zero-Current-Switching - ZCS). In this work, a small-scale prototype was implemented, aiming to obtain a structure capable to operate in a wide range of line frequencies, without requiring any additional complex techniques. In this regard, the developed structure is capable to work as a Power Factor Correction (PFC) stage in a wide range of input frequencies (30Hz - 120Hz) with a Total Harmonic Distortion of the input current (THD_i) of less than 2.19%.**

***Keywords* – Boost Converter, Discontinuous Conduction Mode (DCM), Frequency Variations, Half-Controlled, High Power Factor, MEA, Multipulse Converter.**

I. INTRODUCTION

Currently, three-phase AC/DC converters have a wide range of applications for high power systems, such as adjustable-speed drive (ASD), all-electric ships (AES), data centers, power supply for aircraft, wind power plants and, applications in direct current transmission, induction heating, among others. The AC/DC conversion process can be carried out using several techniques and equipment, however, for this process not to lead to the degradation of the Power Factor (PF), standards are established to maintain the power quality of the grid [1], [2].

Among the methodologies employed in Power Factor Correction (PFC), to attend to these power quality requirements, are the use of transformers/autotransformer with phase shift associated to bridge rectifiers, which are known as Multipulse Converters [3]–[6]. The main idea of the use of these converters is to take advantage of the angular displacement, provided by the transformers/autotransformers so that the cancellation of certain harmonic components occurs. In general, it is observed that the higher the order of the Multipulse Converters, the lower the characteristic harmonic content of the structure. However, this change usually implies a greater complexity in the transformers' winding construction, as well as greater weight and volume of the final structure.

A possible alternative, in order to avoid the employment of transformers with higher orders, and consequently having more complex windings, is the integration of an active structure, such as a half-controlled (also known as bridgeless) converter (HCC) based on Boost topology, to the traditional 12-pulse rectifier, which allows minimizing the harmonic content presented by the structure and reducing the number of elements conducting in each operation stage [7]. This integration aggregates greater flexibility in the adjustment of the output voltage, which changes not only according to the magnitude of the grid voltage, but also to the duty cycle (D) of the converter and, because it does not employ two controlled switches on the same branch it does not incur the risk of a short circuit on it, making its control and operation simpler.

Although this integration adds some advantages, even with great efforts because of the use of control techniques and synchronization algorithms (PLL), it was verified, the difficulty in order to shape a sinusoidal waveform to the current signal [8]–[10].

During the design stage of the HCCs structures, two main strategies are possible: Operate in continuous conduction mode (CCM) or discontinuous conduction mode (DCM). Choosing the operation mode of the converter to be incorporated is of paramount importance in the specifications of its parameters. In this manner, it is observed that the operation in CCM entails great difficulties in modulating the negative half-cycle of the current, which results not only in significant Total Harmonic Distortion of the input current

Manuscript received 05/17/2021; first revision 09/19/2021; accepted for publication 11/01/2021, by recommendation of Editor Demercil de Souza Oliveira Jr. http://dx.doi.org/10.18618/REP.2021.4.0017

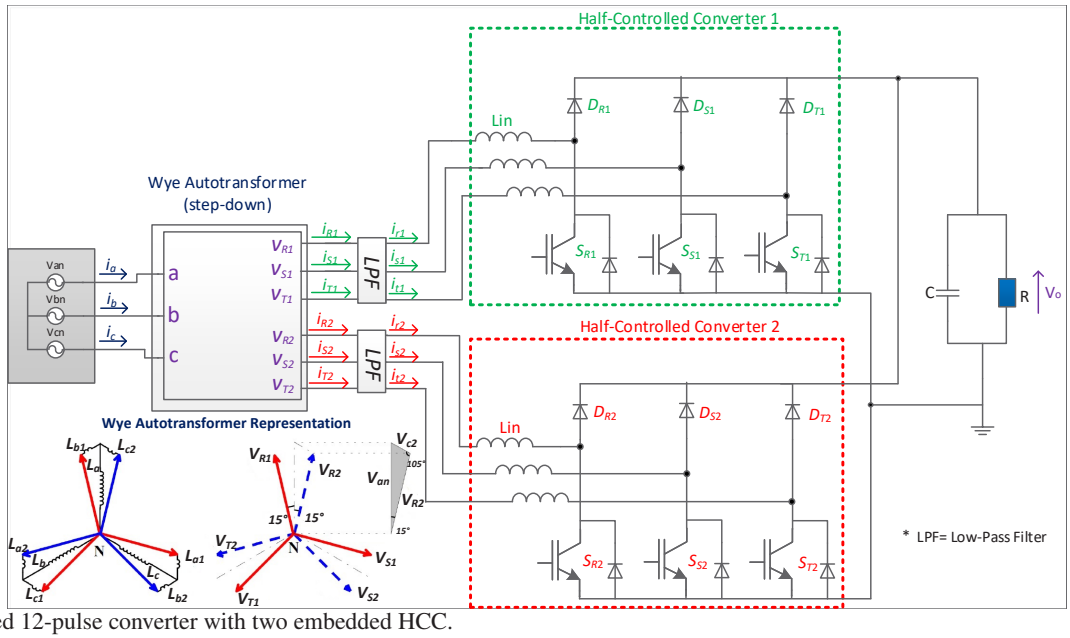

Fig. 1. Proposed 12-pulse converter with two embedded HCC.

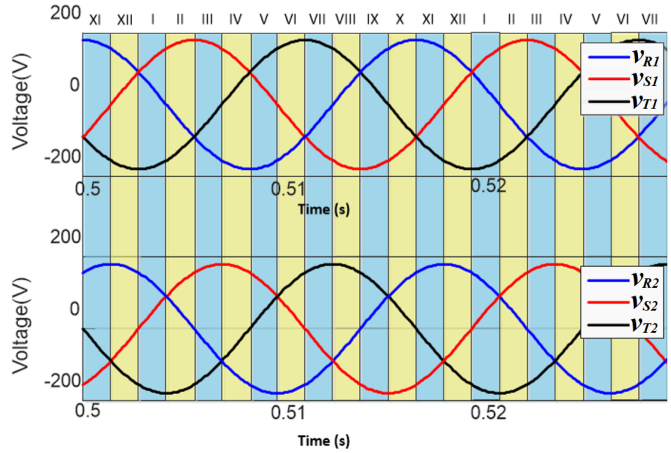

Fig. 2. Operation sectors.

(THD$_i$) but also in the presence of even-order harmonic components. This set of characteristics hinders the mitigation of harmonic content and requires a control circuit of greater cost and complexity [8].

The option of operating in the DCM, in turn, presents a favourable characteristic for applying active correction of the power factor: At the end of the switching period, all the energy stored in the inductor is supplied to the load, so that the peak value of the current over the inductor will be proportional to the applied voltage. In other words, the peak of input current naturally tends to follow the input voltage in the discontinuous conduction mode and the switch will begin to conduct with the current value equals to zero, i.e., it will present the ZCS (Zero Current Switching) characteristic, reducing the switching loss.

The incorporation of the HCC operating in the DCM to the traditional 12-pulse rectifier allows taking advantage of the angular displacement, canceling the most significant harmonic components presented by the structure (5^{th} and 7^{th}) in this mode of conduction [9], as well as to reduce the complexity of the control circuit, making possible the operation even in an open-loop, commanding all active switches by the same control signal [11].

The 12-pulse converter with two embedded HCC, shown in Figure 1, presented in computational analysis a THD$_i$ of 1.73%, significantly below the 14% reported by the one without the active switches, which allows concluding that the incorporation of HCC can be an alternative to increase the order of pulses, resulting in harmonic content reduction, without incurring a significant increase in the weight, volume and complexity of the final structure [11]. In general, the operation in DCM has the dealing with higher values of peak current in the switches as a downside [12], [13]. The proposed structure, on the other hand, by employing six branches, divides the current stress among each one of them, making the operation in DCM a suitable solution.

The replacement of pneumatic, hydraulic, and mechanical systems with electrical systems has been a trend in more electric aircraft (MEA) and can provide a weight reduction up to 10% and a consumption reduction of up to 9% [14]–[16]. The MEA concept has required equipment to operate at growing powers and that are reliable, safe, provides good performance and can operate in faulty conditions [15]. Another challenge provided by applications such as MEA lies in the fact of dealing with a wide range of power frequency variation (360 - 800 Hz) [14]. Similarly, in wind turbines (WECS), although it is possible to operate in fixed frequencies, those that can operate in the whole range (0 - 100%) obtain better efficiency rates in the conversion of wind energy into electrical energy [17].

This paper aims to continue the research proposed by [11], by implementing a small-scale prototype and pushing the state of art further, adding the analysis of the impact of power supply frequency variations (30Hz - 120Hz) in the input current waveform. The possibility of working in a wider range of power supply frequencies combined with its structural advantages make the 12-pulse HCC-embedded converter more attractive for applications with higher requirements for input current harmonic content, meeting, for example, the THD$_i$

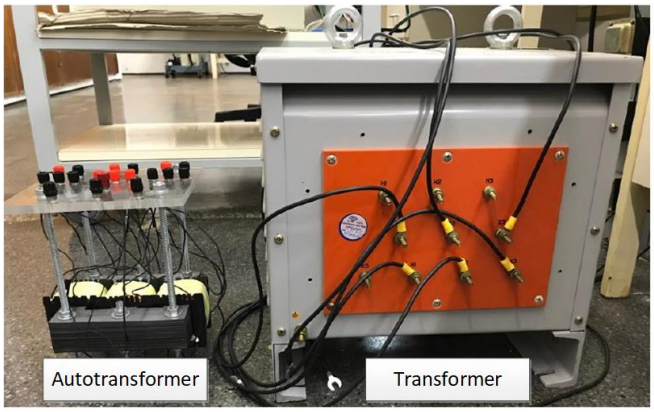

Fig. 3. 12-Pulse Autotransformer vs 12-Pulse Transformer (Size).

criteria established in MIL-STD-704F (for aircraft) [14], [18]. Additionally, it is worth mentioning that the usage of an autotransformer configuration, instead of a transformer, makes possible a significant reduction of the size and weight of the final structure since it processes around one-fifth of total magnetic flux processed by the isolated transformer [19]. In Figure 3 is shown the comparison between the sizes of the autotransformer (analyzed in this paper) and a transformer, both designed to operate at the same output power.

II. PROPOSED 12-PULSES CONVERTER WITH 2-HCCS

In this section the main considerations for the design of the 12-pulse converter with two embedded HCC are presented. As commented, when the proposed structure operates in discontinuous conduction mode provides a series of advantages, once at each end of switching period all the energy stored in the inductor is transferred to the load, i.e., by employing a fixed duty cycle and a switching frequency, significantly greater than grid's voltage frequency, the inductor peak current will be proportional to its voltage, allowing the structure to act as a PFC device without the need for any current control circuitry or current sensing.

In this regard, so as to properly design a converter, it is necessary to address two main issues: Specify the inductor value to guarantee the discontinuous conduction mode; Comprehend the operation stages of the converter. Among the elements that constitute the proposed converter is the twelve-pulses phase shift autotransformer, at low kVA rating, responsible to provide two sets of three-phase secondary windings, displaced by 30^o from each other, as shown in Figure 1. The proposed structure takes advantage of the phase shift provided by this autotransformer to cancel the lower order current harmonics (5^{th} and 7^{th}) on the primary side.

Once the phase-shift, provided by the 12-pulse autotransformer, cancels the lower order harmonics, the low-pass filters (L_fC_f) shown in Figure 1, have a cutoff frequency equals to one-tenth of the switching frequency (f_s), being responsible to cancel the switching harmonics, making possible to reduce the size of its elements. Thus, the set of voltages that supply both HCC structures are shown in Figure 2, resulting in 12 cyclically repeated operating sectors (I - XII).

By analyzing the Figure 2 (Operation sectors), one should notice that each one of the sectors is delimited by one crossing voltage, e.g., the transition from Sector X to Sector XI is delimited by v_{T2} crossing from a positive value to a negative one. Once each one of these sectors has its own operation stages, which significantly increases the total number of stages of this structure. For a better understanding of how the secondary voltages affect the operation stages, let us take Sector X as an example.

Thus, the following analysis presents two transition stages named as "beginning" (transition between Sectors IX and X) and "ending" (transition between sectors X and XI), and the third stage in which all voltages in the secondary winding have a non-null value, named as "Sector X". This analysis neglected the small variations on the secondary voltage during the switching period (T_s).

Beginning: During the charging stage (DT_s) show in Figure 4.a, although the same control signal was sent to all controlled switches (same control signal to both HCC1 and HCC2), the voltage v_{T1} has null voltage during this stage, resulting in a null current in the elements connected to its branch. Thus, the charging stage for HCC1 will happen as follows: The switch S_{R1} is directed polarized and has received the control signal, making a positive current flowing through L_{R1}, and returning through L_{S1}. With regard to HCC2 the voltages v_{R2} and v_{T2} are positive, making respectively switches S_{R2} and S_{T2} directed polarized and two currents i_{r2} and i_{t2} flowing through these switches and returning by the diode connected to L_{S2}, which is connected to a secondary winding having a negative voltage.

During the discharging stage, all energy stored in the inductors will be transfer to the load, and the output capacitor (C). The equivalent circuitry for this stage is shown in Figure 4.b. Once the energy stored in the inductors is transferred, a dead time will occur as shown in Figure 4(g).

During Sector X: During this stage, all secondary windings have a non-null voltage, i.e., every branch of both HCC's will have one semiconductor (controlled switch or diode) conducting during the charging stage (DT), whose equivalent circuitry is shown in Figure 4.c, and its discharging stage is shown in Figure 4.d. Once the proposed converter operates in DCM, analogously to the previous case, after the discharging stage, all inductors will have null current and its circuitry will be as shown in Figure 3(g).

Ending: At the ending stage, the v_{T2} voltage has a null-value therefore, the HCC2 will present a behavior likewise the one present by HCC1 at "the beginning", having three operational stages shown in Figures 4.e to 4.g. By analyzing Figure 2 (Operation sectors) it is possible to evaluate the moments when each HCC structure is subject to the maximum voltage (line voltage) and, once it acts as a PFC, when it is subject to the maximum current, providing means to the designer to specify the inductor present on them.

Taking the transition between Sector VI to VII, the v_{T1} voltage is in its maximum value and both v_{R1} and v_{S1} have the same value and opposite signal of v_{T1}, thus the equivalent circuitry for the charging stage (DT_s) for those conditions is shown in Figure 5.a. Additionally, by neglecting the non-idealities of the switches, one should obtain the equivalent circuit shown in Figure 5.b, where an equivalent inductance (L_{boost}) for an HCC, under these conditions, may be expressed

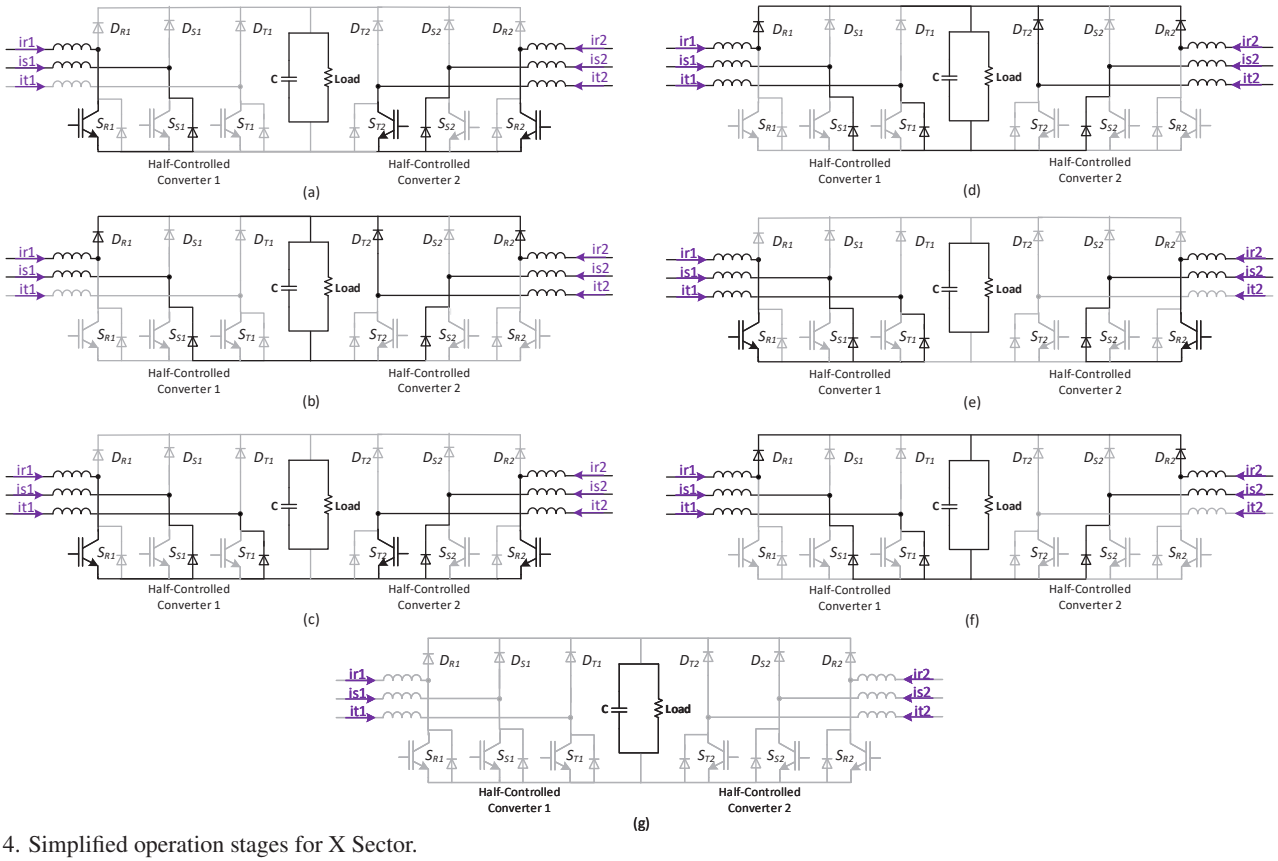

Fig. 4. Simplified operation stages for X Sector.

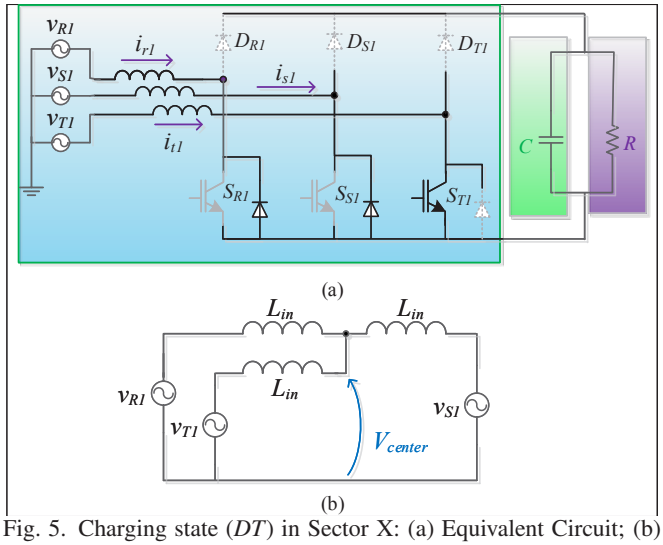

Fig. 5. Charging state (DT) in Sector X: (a) Equivalent Circuit; (b) Simplified Circuit.

as follows in (1).

$$L_{boost} = \frac{3}{2} L_{in}. \tag{1}$$

Once this converter operates as a PFC, the current in each inductor is proportional to the voltage applied to it, making the instant of maximum voltage also the instant of maximum current. Considering the set of voltages supplying both HCC's, and the characteristics described, the currents in the inductors will follow (2) and (3).

$$i_{r_1}(t) + i_{s_1}(t) + i_{t_1}(t) = 0. \tag{2}$$

$$i_{r_2}(t) + i_{s_2}(t) + i_{t_2}(t) = 0. \tag{3}$$

Even so, to providing flexibility in the regulation of the output voltage (by adjusting the duty cycle), the proposal of the structure also adds the possibility of using a very simpler control logic, to deal with power supply frequency variations, although this does not imply a compulsory requirement. Among the possible logic, the same pulse (without any discrepancies) can be sent to all active switches, simultaneously, with no degradation of the input current parameters.

To design the inductors, first, it is desirable to understand how the operation steps of the converter are obtained. Considering the characteristics of the power system, the converter features 12 cyclically repeating sectors, as shown in Figure 2, each one enabling a set of operation steps, that are shown in Figure 4.

The delimitation of the sectors is given when there is the reverse direction of one of the voltages that occurs in the secondary winding. The sectors are listed sequentially from I to XII. It should noticed that the switching period T_s is much smaller than a given sector duration (e.g. Sector X), thus the stages of a converter working in DCM will be seen multiple times in every given sector.

Another important issue is that the value of the voltage varies during the sectors, e.g., voltage V_{T2} starts with a positive value, at the beginning of Sector X, and at the end has its value equal to zero, which add more possible operation steps (like

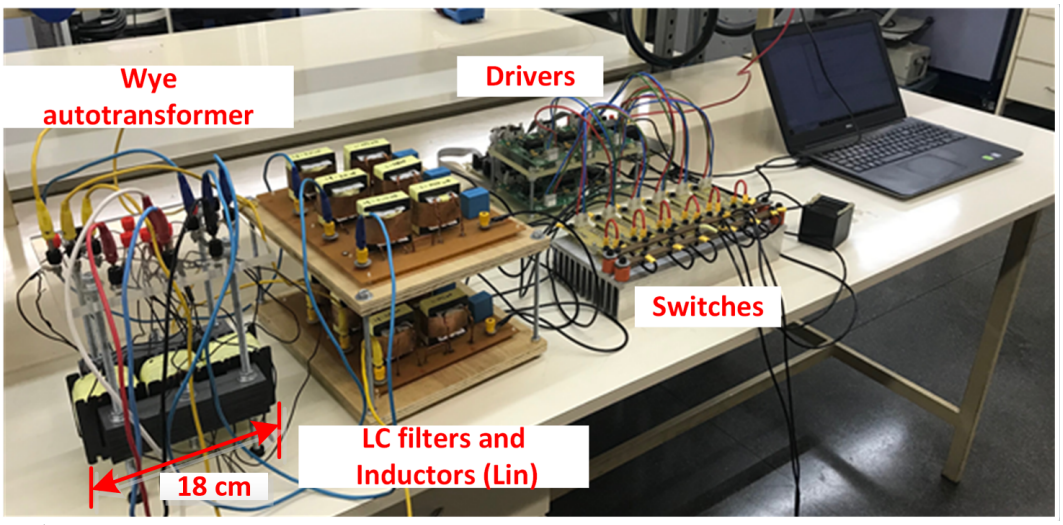

Fig. 6. Experimental set-up.

the ones shown in Figure 4) in this sector.

Considering the number of sectors, to analyze the operation steps, Sector X was taken as an example. By analyzing the steps (a) to (g) presented in Figure 4, a good understanding of the converter operation is obtained. It should be noted that the converter acts as PFC, so the voltage v_{R1} and the envelope of the current i_{r1} have the same phase.

To properly specify the inductors for the set of cyclically repeated conditions, one should consider two main issues: The maximum line voltage applied to the HCC's ($V_{L_{pk}}$) and the peak value of inductor current (I_{pk}). The parameter α is determined by the quotient between the peak value of line voltage ($V_{L_{pk}}$) with the output voltage (V_o) as shown in (4):

$$\alpha = \frac{V_{Lpk}}{V_o}. \tag{4}$$

During the charging stage, each HCC is compound by a set of three inductors that will be storing energy. To ensure that they will operate in DCM, the design of the inductance must consider the maximum value of the current in this set of inductors. Thus, the inductance L_{in} must obey (5).

$$L_{in} < \frac{2}{3}\frac{{V_{Lpk}}^2}{2\pi f_s \frac{P_o}{2}}\frac{(1-\alpha)^2}{\alpha}\sqrt{3\left(Y_o(\alpha)^2\right)}. \tag{5}$$

Where P_o is the output power, f_s is the switching frequency and the Y_o is determined by (6).

$$Y_0(\alpha) = -2 - \frac{\pi}{\alpha} + \frac{2}{\alpha\sqrt{1-\alpha^2}}\left(\frac{\pi}{2} + \tan^{-1}\left(\frac{\alpha}{\sqrt{1-\alpha^2}}\right)\right). \tag{6}$$

III. EXPERIMENTAL RESULTS

Some power applications, such as MEA (More Electric Aircrafts), must deal with a wide range of power supply frequencies at the same time they have to meet to the THD_i standards. Having these criteria into account, this section aims to verify if the proposed structure presents itself as a suitable solution for applications which requires the possibility to deal with a wide range of power supply frequencies.

For this analysis, the reference was made to an application in which the input frequency varies over a wide range of values. A small-scale prototype was made, shown in Figure 6, operating in the power supply voltage range from 30Hz to 120Hz. The main parameters of the analyzed converter are shown in Table I.

TABLE I
Main Parameters for the Frequency Variation Analysis

Parameter	Value
C - Output capacitor	100 μF
C_f - Low-pass filter capacitance	3.3 μF
L_f - Low-pass filter inductance	2 mH
f_{in} - Input frequency range	30 - 120 Hz
f_s - Switching Frequency	20 kHz
L_{in} - HCC Inductor	200 μH
P - Load power	800 W
R - Equivalent load resistance	200 Ω
P_o - Nominal output power	1400 W
Autotransformer Step-down factor	0.896
V_i - Supply rms phase voltage	84 VAC
V_o - Output voltage	400 VDC
D - Nominal duty cycle	0.33
Branch switches model	SK 35 GAL

The proposal converter employs a Wye step-down autotransformer (auto-connected), which supplies the HCC bridges with 127V (rms line voltage). To verify the behavior of the proposed structure under power frequency variations, all the results presented in Figures 7.a to 7.e employed an 800W load and are displayed at the same time basis, making easier the comparison between the displayed cases.

By analyzing Figures 7.a to 7.e and the detail presented in Figure 7.f, one can see that the structure was able to act as PFC, i.e., the line current presents the waveform very close to a sinusoidal shape (voltage waveform), maintaining its symmetry and appropriate phase displacement, without requiring any adjustment on its parameters (same set-up for

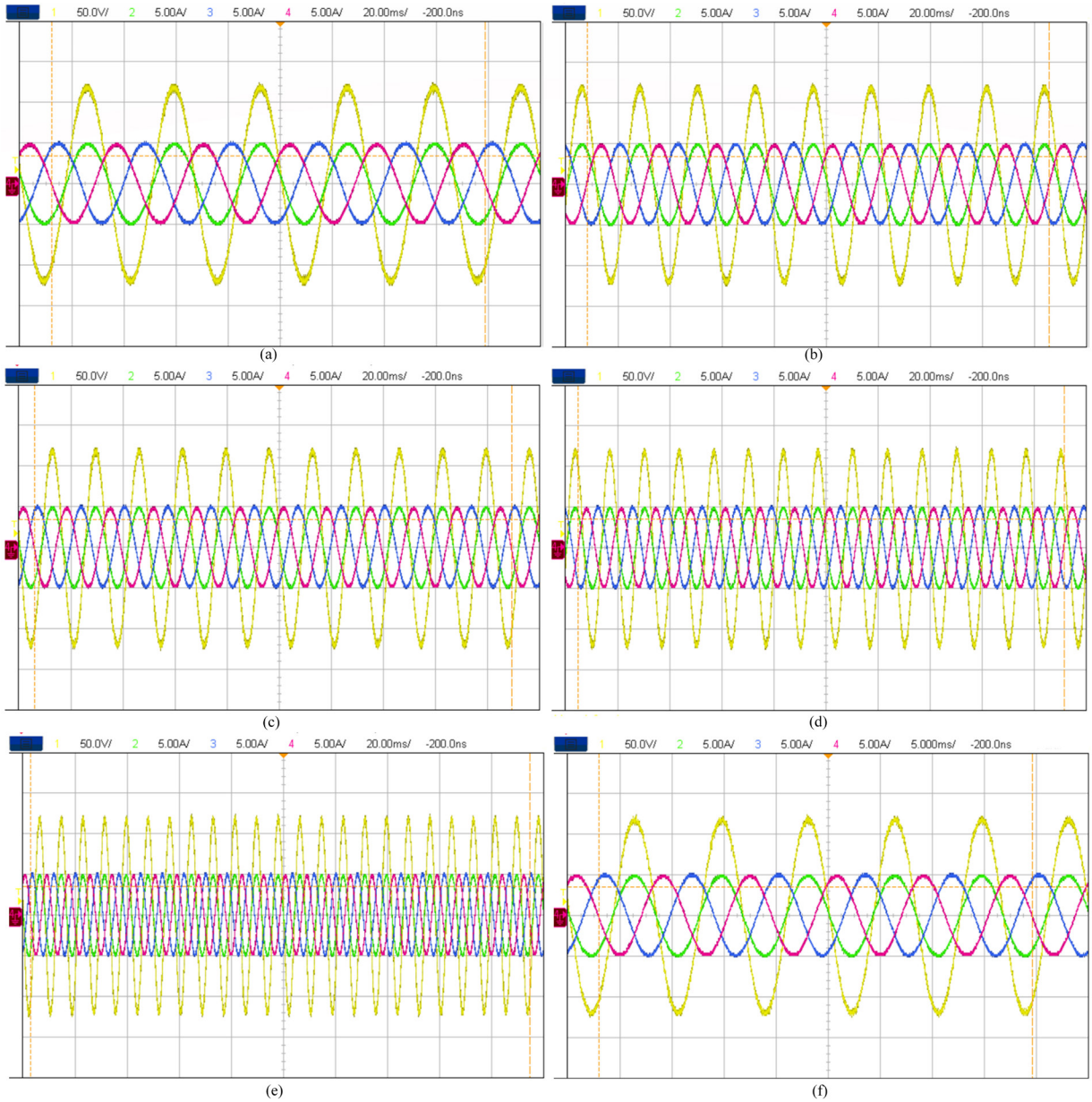

Fig. 7. Main waveforms of at the grid side, for different input frequency. v_{cn} (yellow), i_a (red), i_b (blue), i_c (green): (a) 30Hz; (b) 45 Hz; (c) 60 Hz; (d) 75 Hz; (e) 120Hz; (f) Detail of the 120 Hz waveforms.

all cases).

Due to its characteristics, the proposed converter did not require the use of any current loop control, neither required any phase displacement between pulses. In this regard, the employed control strategy is based on a single-loop voltage control, where the control-to-output transfer function G_{vd} of the proposed structure can be approximated to the traditional three-phase Boost converter transfer function operating in DCM, as described by (7).

$$G_{vd}(s) = \frac{G_{vd0}}{1 + \frac{s}{\omega_p}}. \tag{7}$$

where

$$G_{vd0}(s) = \frac{2V_o}{D}\left(\frac{M-1}{2M-1}\right). \tag{8}$$

$$\omega_p = \frac{2M-1}{(M-1)RC}. \tag{9}$$

and M is the static gain in DCM, expressed by (10).

$$M = \frac{1 + \sqrt{1 + \frac{4RD^2}{f_s L_{boost}}}}{2}. \tag{10}$$

Thus, from Table I, the bode diagram of the transfer function G_{vd}, including the gain sensor $H = 2.5/400$ V/V, is illustrated in Figure 8 (curve blue in color). Then, a PI controller was adopted for the control design and, as shown in Figure 8 (yellow in color), by using a proportional gain K_p = 0.09 and an integral gain K_i=38.34, a crossover frequency f_c = 20Hz and phase margin $PM = 86°$ are achieved from the open-loop voltage control.

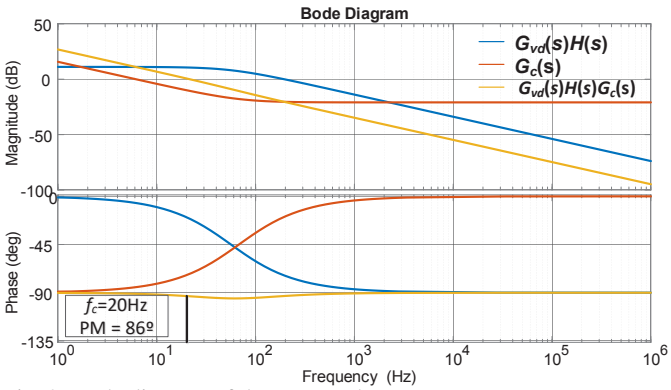

Fig. 8. Bode diagram of the proposed converter.

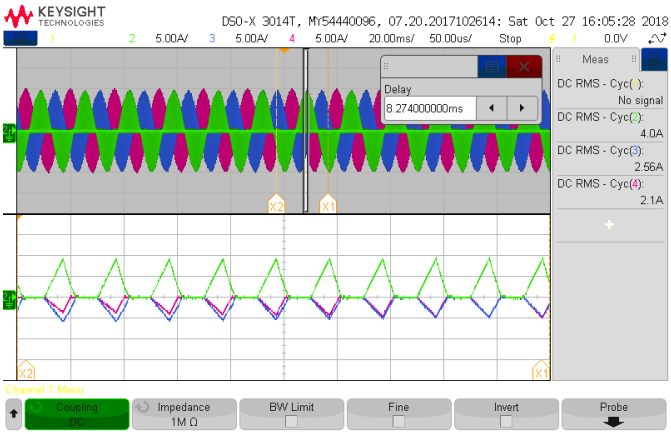

Fig. 9. Waveforms of the currents i_{r1} (blue), i_{s1} (red), i_{t1} (green) for 60Hz input frequency and the detail of the waveforms when the maximum value of i_{t1} occurs.

It should be noted that the cutoff frequency of the LC filter is one-tenth of f_s (the switching frequency is equal to 20 kHz). The employed autotransformer is responsible to cancel the 5^{th} and 7^{th} order harmonics, thus, the LC filter is not as bulky as those commonly employed in traditional 12 pulse converters. Once the waveform of the grid currents is obtained, it should verified the behavior of the currents i_{r1}, i_{s1}, and i_{t1}. The waveforms for a 60Hz input frequency, are shown in Figure 9.

By analyzing Figure 9 one can see that in fact, the inductors currents obey the logic expressed in (2) and (3), in other words, at a given moment the sum of the currents belonging to the same HCC is equal to zero. Comparing Figure 9 and Figure 10, one should notice that after the LC filter influence, the currents in the secondary winding are not pulsed but their waveform although closer to a sinusoidal wave, still have some harmonic components (mainly the 5^{th} and 7^{th} harmonics).

The waveforms of the currents i_{R1}, i_{S1} and i_{T1} are shown in Figure 10 along with the grid line voltage v_{ST}. It is important to note that although the phase supply voltage (V_i) is equal to 84V, because the configuration employed (Wye step-down), the rms value of the line voltage (V_L) in the secondary will respect (11).

$$V_L = V_i\sqrt{3}\,(0.896)\,. \tag{11}$$

Once the main waveforms of the converter were shown, it is desired to verify how the curve relating the harmonic

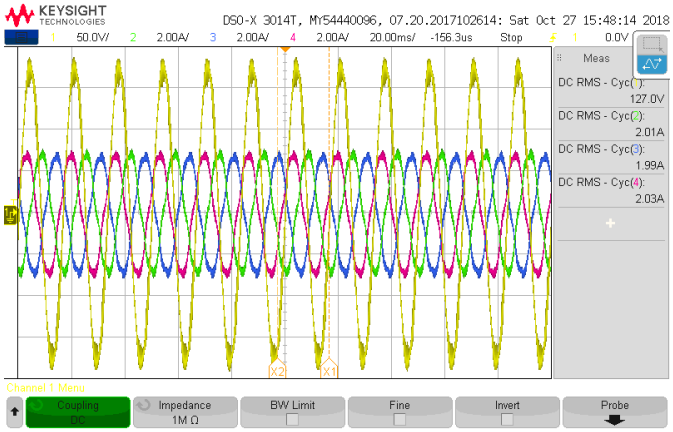

Fig. 10. Currents i_{R1} (blue), i_{S1} (red), i_{T1} (green) and v_{ST} (yellow) Voltage.

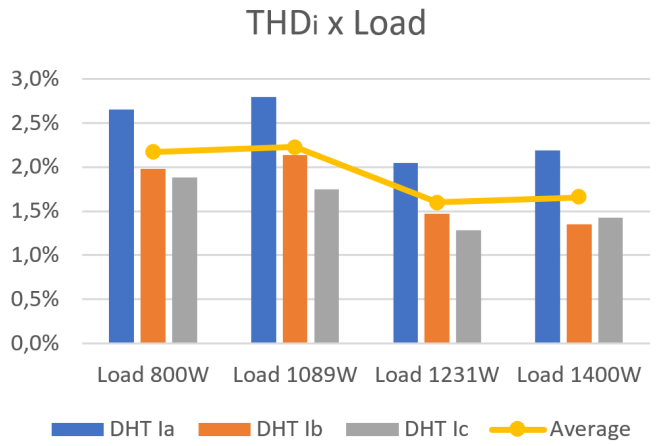

Fig. 11. THD_i behavior vs load power.

distortion and load is given. For this test, the converter was supplied with an input frequency of 60Hz for all measured points. The curve relating THD_i (Total Harmonic Distortion of the current) and Load is shown in Figure 11.

When analyzing the curves shown in Figure 11, it can be verified that the structure presented a significantly reduced harmonic content, 2.19% in nominal conditions (I_a), when compared to the 14% of the traditional structure, also meets the criterion of THD_i of the MIL-STD-704F, which establishes that the THD_i must be below 5%.

IV. CONCLUSION

The results presented in this work allow us to conclude that the 12-pulse converter with embedded HCC bridge presents the possibility of higher power factor operation over a wide power frequency range, using only a single-loop voltage control scheme.

In addition to the possibility of measuring only the output voltage, the driver circuit sends the same command signal to the switches, without the need for phase shift and, due to the structural characteristics of the converter, the active switches are all in the same reference, which corroborates the design simplicity of the command circuitry.

These features, provided by the intrinsic characteristics of the structure, allow the designer to reduce the number of sensors required since there is no need measure the input

currents as well as the reduction of the computational cost, since the structure can operate only with the voltage loop control.

The results presented by the small-scale prototype allow us to conclude that the proposed structure was able to operate, as a PFC, in a wide range of power supply frequencies (30Hz up to 120 Hz), which makes the structure a possible alternative for applications in which the power frequency can vary in a substantially.

Naturally, for each application where it is desired to employ the proposed converter, it is necessary to consider the range of frequencies in which the converter will be subjected since these parameters are directly related to the autotransformer design and, the parameters of the HCC bridges.

When analyzing how the THD_i behavior in function of the load, it can be verified that the structure presents reduced THD_i less than 5% for all analyzed cases. These results allow concluding that the incorporation of the HCC bridges to the 12-pulse autotransformer, is an alternative to the use of higher-order converters, which implies reducing the complexity of the final structure. Besides, by using the autotransformer configuration, the magnetic flux processed by it will be around one-fifth of the one processed by the isolated transformer, resulting in a significant reduction of the weight and size of this element.

Given the numerous features described, such as high robustness, simplicity of design, switch command logic that does not require any sensors, PLL, having all control switches in the same reference and ZCS switching of semiconductors guaranteed, and the possibility to operate with the variable input frequency. The authors understand that this structure can become a strong candidate in three-phase applications with variable frequency, such as Wind Generation, MEA, Electric Traction, among others.

ACKNOWLEDGEMENTS

The authors wish to thank the Federal Institute of São Paulo (Instituto Federal de São Paulo - IFSP), the São Paulo Research Foundation (FAPESP) and the São Paulo State University (UNESP), which provided resources and all the structure that enabled this work to be carried out. This research was supported in part by the Coordenação de Aperfeiçoamento de Pessoal de Nível Superior - Brasil (CAPES) - Finance Code 001 and the São Paulo Research Foundation - FAPESP Grant No. 2015/15872-9.

REFERENCES

[1] IEEE, "IEEE Recommended Practice and Requirements for Harmonic Control in Electric Power Systems", *IEEE Std 519-2014 (Revision of IEEE Std 519-1992)*, pp. 1–29, June 2014.

[2] IEC, "Electromagnetic compatibility (EMC) - Part 3-2: Limits - Limits for harmonic current emissions (equipment input current 16 A per phase)", *IEC 61000-3-2:2018*, pp. 1–73, January 2018.

[3] D. Paice, I. I. A. Society, *Power Electronic Converter Harmonics: Multipulse Methods for Clean Power*, IEEE Press, 1996.

[4] B. Singh, S. Gairola, B. N. Singh, A. Chandra, K. Al-Haddad, "Multipulse AC-DC Converters for Improving Power Quality: A Review", *IEEE Transactions on Power Electronics*, vol. 23, no. 1, pp. 260–281, January 2008.

[5] S. P. P., R. Kalpana, B. Singh, G. Bhuvaneswari, "A 20-Pulse Asymmetric Multiphase Staggering Autoconfigured Transformer For Power Quality Improvement", *IEEE Transactions on Power Electronics*, vol. 33, no. 2, pp. 917–925, February 2018.

[6] D. L. Mon-Nzongo, P. G. Ipoum-Ngome, T. Jin, J. Song-Manguelle, "An Improved Topology for Multipulse AC/DC Converters Within HVDC and VFD Systems: Operation in Degraded Modes", *IEEE Transactions on Industrial Electronics*, vol. 65, no. 5, pp. 3646–3656, May 2018.

[7] Y. Wang, D. Panda, T. A. Lipo, D. Pan, "Performance improvement of dual-half-controlled-converter and its applications in utility rectifiers", *in 8th International Conference on Power Electronics - ECCE Asia*, pp. 1711–1718, 2011.

[8] M. M. Reis, B. Soares, L. H. S. C. Barreto, E. Freitas, C. E. A. Silva, R. T. Bascope, D. S. Oliveira, "A variable speed wind energy conversion system connected to the grid for small wind generator", *in 2008 Twenty-Third Annual IEEE Applied Power Electronics Conference and Exposition*, pp. 751–755, 2008.

[9] D. S. Oliveira, L. H. S. C. Barreto, F. L. M. Antunes, M. I. B. V. Silva, D. L. Queiroz, A. R. Rangel, "A DCM three-phase high frequency semi-controlled rectifier feasible for low power WECS based on a permanent magnet generator", *in 2009 Brazilian Power Electronics Conference*, pp. 1193–1199, 2009.

[10] D. S. Oliveira, Jr., M. M. Reis, C. E. A. Silva, L. H. S. Colado Barreto, F. L. M. Antunes, B. L. Soares, "A Three-Phase High-Frequency Semicontrolled Rectifier for PM WECS", *IEEE Transactions on Power Electronics*, vol. 25, no. 3, pp. 677–685, March 2010.

[11] J. C. Pelicer, F. J. M. de Seixas, A. C. de Lourenço, L. Silva, "Novel isolated multi-pulse rectifiers with low current distortion using three-phase half-controlled boost converters", *in 2015 IEEE 13th Brazilian Power Electronics Conference and 1st Southern Power Electronics Conference (COBEP/SPEC)*, pp. 1–5, 2015.

[12] M. H. Granza, R. Gules, C. H. Illa Font, "Hybrid and Three-Level Three-Phase Rectifiers Using Interleaved DCM Boost Converters", *IEEE Access*, vol. 7, pp. 160168–160176, November 2019, doi:10.1109/ACCESS.2019.2951123.

[13] S. Gangavarapu, A. K. Rathore, "Three-Phase Buck-Boost Derived PFC Converter for More Electric Aircraft", *IEEE Transactions on Power Electronics*, vol. 34, no. 7, pp. 6264–6275, July 2019, doi:10.1109/TPEL.2018.2877509.

[14] J. Chen, X. Zhang, C. Wen, "Harmonics Attenuation and Power Factor Correction of a More Electric

Aircraft Power Grid Using Active Power Filter", *IEEE Transactions on Industrial Electronics*, vol. 63, no. 12, pp. 7310–7319, December 2016.

[15] K. Rajashekara, "More Electric Aircraft Trends [Technology Leaders]", *IEEE Electrification Magazine*, vol. 2, no. 4, pp. 4–39, December 2014.

[16] J. Benzaquen, M. B. Shadmand, A. Stonestreet, B. Mirafzal, "A unity power factor active rectifier with optimum space-vector predictive DC voltage control for variable frequency supply suitable for more electric aircraft applications", *in 2018 IEEE Applied Power Electronics Conference and Exposition (APEC)*, pp. 1455–1460, 2018.

[17] V. Yaramasu, B. Wu, P. C. Sen, S. Kouro, M. Narimani, "High-power wind energy conversion systems: State-of-the-art and emerging technologies", *Proceedings of the IEEE*, vol. 103, no. 5, pp. 740–788, May 2015.

[18] D. of Defense, "AIRCRAFT ELECTRIC POWER CHARACTERISTICS", *MIL-STD-704 Rev F*, March 2004.

[19] F. J. M. d. Seixas, *Conversores CA-CC de 12 KW com elevado fator de potencia utilizando autotransformador com conexao diferencial de multiplos pulsos*, Ph.D. thesis, Universidade Federal de Santa Catarina, Centro Tecnologico. Programa de Pos-Graduacao em Engenharia Eletrica, 2001.

BIOGRAPHIES

João Carlos Pelicer Junior, was born in São Paulo, SP, Brazil, in 1989. He received a B.S. degree in Electrical Engineering from São Paulo State University (UNESP) in 2012, where he also obtained M.S. and Ph.D. degrees in 2014 and 2019, respectively. He is currently a Professor at the Federal Institute of São Paulo (IFSP). His research interest includes high-power factor rectifiers, multipulse converter applications, power factor correction, and switching converters.

Angelo César de Lourenço, was born in Maringá, Brazil, in 1976. He received a B.S. degree in Electrical Engineering from the Federal University of Mato Grosso do Sul, UFMS, Campo Grande, in 1998, the M.S. degree in Electrical Engineering from Universidade Estadual Paulista, UNESP in 2001, where he also obtained a Ph.D. in 2016. Currently he is a Professor at the Federal Institute of Mato Grosso do Sul, IFMS, Campo Grande since 2010. His research interests include electrical power factor correction, renewable energy, electric machines and drives.

Luis De Oro Arenas, was born in Cartagena de Indias, Colombia. He received the B.Sc. degree in electronic engineering from the National University of Colombia, Bogotá D.C., Colombia, in 2012, and the M.Sc. and Ph.D. degrees in electrical engineering from São Paulo State University (UNESP), Ilha Solteira (SP), Brazil, in 2014 and 2019, respectively. He is currently a postdoctoral fellow with the Group of Automation and Integrated Systems, São Paulo State University (UNESP), Sorocaba (SP), Brazil. His current research interests include power electronics, power quality, power theories, smart-metering, and microgrids.

Falcondes José Mendes de Seixas, was born in Jales, SP, Brazil. He received the B.S. degree in electrical engineering from the Engineering School of Lins, Lins, Brazil, in 1988 and the M.S. and Ph.D. degrees in electrical engineering from the Federal University of Santa Catarina, Florianpolis, Brazil, in 1993 and 2001, respectively. He is currently an Assistant Professor at the Department of Electrical Engineering, São Paulo State University (UNESP), Ilha Solteira, Brazil. His research interests include high-power factor rectifiers, three-state switching cell and multi-pulse converter applications.